Mechanisms of discrete- and continuous-spectrum generation and weakly and strongly asymmetric modes in a superradiant laser with a low-Q combined cavity

© E.R. Kocharovskaya[1], Vl.V. Kocharovsky[1,2]

[1] Institute of Applied Physics, Russian Academy of Sciences,
Nizhny Novgorod, Russia
[2] Lobachevsky State University,
Nizhny Novgorod, Russia
E-mail: katya@appl.sci-nnov.ru

Received April 15, 2024
Revised June 20, 2024
Accepted June 20, 2024

Using the Maxwell–Bloch equations in the case of homogeneous broadening of spectral line of a two-level active medium placed in a low-Q combined Fabry-Perot cavity with identical mirrors and distributed feedback of counterpropagating waves, numerical simulations of a non-stationary (single- and multi-mode) asymmetric superradiant lasing are carried out. It is established that, in the general case, laser radiation is not mirror-symmetric and its spectrum contains discrete and continuous components. The main mechanisms of their origin are clarified and, using a number of examples, the possibility of simultaneous generation of one powerful, strongly asymmetric, polariton mode in the center of the spectral line and several weaker, almost symmetrically emitting, polariton modes (harmonics) outside it is demonstrated.

Keywords: superradiant laser, population-inversion grating, polariton modes, self-modulation, discrete spectrum, continuous spectrum, low-Q combined cavity, distributed feedback.

DOI: 10.61011/SC.2024.04.58849.6356H

1. Introduction

The self-modulation and spectrum of superradiant lasers, even with a homogeneous broadening of spectral line of a two-level active medium, are determined not only by the interaction of the modes of the electromagnetic field of the cavity $E(z,t)$ due to the known quadratic nonlinearity of saturation of this medium [1–5]. First of all, the nature of the generated radiation is determined by the consistent space-time dynamics of the polarization $P(z,t)$, i.e., the density of optical dipole moments of active centers, and the inversion of the populations of the energy levels of these centers $D(z,t)$. The non-standard hierarchy $T_E \ll T_2 \lesssim T_1$ of times of incoherent relaxation of the field, polarization and inversion of energy-level population, respectively, ensures the occurrence of new features of single-mode self-modulation and multimode laser dynamics described by the semi-classical Maxwell–Bloch equations for such lasers, unlike traditional lasers (see, for example, [4–7]).

One of these effects is associated with the half-wavelength grating [5–7] of population inversion formed by counterpropagating waves in a combined Fabry-Perot cavity with distributed feedback (FP-DFB). This grating non-linearly changes the Q-factor of the laser polariton modes, initially set by the cavity, which is low-Q one according to the definition of a superradiant laser. Even in the case of a symmetrical cavity considered below, the grating can be mirror-asymmetric and result in an asymmetric radiation.

Near the generation threshold, the laser polariton mode is usually stationary and has a very narrow spectrum with a width less than $T_2^{-1} \ll T_E^{-1}$. When the laser threshold is not very much exceeded, superradiant generation, as a rule, is still attributable to a single polariton mode at a frequency near the center of the spectral line of the active medium ω_{21}, but has a nonlinear inhomogeneous structure that differs from the one set by the FP-DFB cavity due to Bragg scattering and simultaneous amplification on the specified grating, and may be subject to regular self-modulation. When the threshold is greatly exceeded, the laser dynamics can become complex and irregular depending on the laser parameters, resulting in an asymmetric coherent radiation with several time scales and various features of the discrete and continuous spectrum. Such a complicated lasing is characteristic of active media, including semiconductors, with a rather weak inhomogeneous broadening of the spectral line of superradiant active centers, for example, impurities, excitons, electrons and holes in magnetized quantum wells, electrons in quantum cascade lasers, atoms in optical traps [8–14].

This paper is devoted to the analysis of a number of mechanisms responsible for the formation of this kind of radiation, which is not typical for conventional lasers, based on the numerical solution of nonlinear and linearized Maxwell–Bloch equations. Having specified the laser model in the section 2, we briefly characterize the key mechanisms of self-modulation that we found in section 3. The parameters of the lasers are also given there, for which the results of demonstration calculations of dynamics and spectra at different pump levels are provided in the following sections 4 and 5. The conclusion contains general comments and open questions.

2. A model of a superradiant laser with a symmetric cavity

The dynamics of the state of a distributed system of two-level active centers with a transition frequency of ω_{21} and a dipole moment of d in the presence of continuous-wave (CW) incoherent pumping in the cavity FP-DFB is described by the semi-classical Maxwell–Bloch equations [6,7]. The electromagnetic field and the polarization of the medium (the density of optical dipole moments) in them are represented as a pair of counterpropagating waves with smoothly varying complex amplitudes:

$$E = Re\big[A_+(z,t)\exp(ik_0z - i\omega_0 t) + A_-(z,t)\exp(-ik_0z - i\omega_0 t)\big]/\sqrt{\varepsilon_0}, \quad (1)$$

$$P = Re\big[P_+(z,t)\exp(k_0z - i\omega_0 t) + P_-(z,t)\exp(-ik_0z - i\omega_0 t)\big]\sqrt{\varepsilon_0}. \quad (2)$$

The carriers selected are the DFB Bragg frequency ω_0 (for certainty coinciding with the partial frequency of one of the modes of the Fabry-Perot cavity with a real reflection factor of mirrors R) and the associated wave number

$$k_0 = \omega_0 c^{-1}\sqrt{\varepsilon_0}, \quad (3)$$

which is determined by the half-wave length period $\lambda_0/2 = \pi/k_0$ of modulation of the laser waveguide or equivalent modulation of the dielectric constant of the active medium matrix with an effective amplitude b_p (ε_0 is the average value of this dielectric constant, c the speed of light in vacuum):

$$\varepsilon_M = \varepsilon_0 Re\big[1 + 4b_p\exp(2ik_0z)\big]. \quad (4)$$

The population inversion of two-level active centers in the equations is represented as the sum of a smoothly inhomogeneous component $n(z,t)$ and a half-wavelength grating $n_z(z,t)$:

$$D(z,t) = n(z,t) + \mathrm{Im}\big[n_z(z,t)\exp(2ik_0z)\big]. \quad (5)$$

The temporal and spatial scales of the collective behavior of the superradiant system of active centers are set by the cooperative frequency

$$\nu_c = \sqrt{\frac{2\pi d^2\omega_{21}N_0}{\varepsilon_0\hbar}} \quad (6)$$

and the cooperative length $B_c = c/\nu_c\sqrt{\varepsilon_0}$ (N_0 is a concentration of active centers, $\hbar$ Planck's constant). These values are used for the normalization of all frequency, time and space quantities: spectral detuning $\Delta = (\omega - \omega_0)/\nu_c$, the rates of incoherent field relaxation, population inversion and polarization $\Gamma_{E,1,2} = 1/(\nu_c T_{E,1,2})$, laser length $L = B/B_c$ (it is assumed that the length B is a multiple of $\lambda_0/2$), time $\tau = \nu_c t$ and coordinate $\xi = z/B_c$. The dimensionless amplitude of the dielectric-constant modulation $\beta = b_p\omega_0/\nu_c$ serves as the coupling coefficient of the counterpropagating field waves (the DFB coefficient). It is convenient to normalize the amplitudes of polarization and field waves per active center: $p_\pm = P_\pm/(dN_0)$, $\alpha_\pm = A_\pm/(2\pi dN_0) = dA_\pm/(\hbar\nu_c\varepsilon_0)$.

The space-time dynamics of the field is given by Maxwell equations:

$$\left[\frac{\partial}{\partial\tau} + \frac{\partial}{\partial\xi}\right]\alpha_+ + i\beta\alpha_- = ip_+,$$

$$\left[\frac{\partial}{\partial\tau} - \frac{\partial}{\partial\xi}\right]\alpha_- + i\beta^*\alpha_+ = ip_-. \quad (7)$$

Below, for certainty, it is assumed that the DFB coefficient is a real-valued parameter, $\beta = \beta^*$. The components of population inversion obey Bloch's optical equations:

$$\left[\frac{\partial}{\partial\tau} + \Gamma_1\right](n - n_p) = \mathrm{Im}\big[\alpha_+p_+ + \alpha_-p_-\big],$$

$$\left[\frac{\partial}{\partial\tau} + \Gamma_1\right]n_z = \alpha_-^*p_+ - \alpha_-p_-^*. \quad (8)$$

Note that the change of the first, smoothly inhomogeneous component, is determined by the work of the electromagnetic field on the polarization of each of the two counterpropagating waves independently, and the change of the second, grating component is determined by the cross interaction of the forward and backward waves of the field and polarization, ensuring a half-wavelength spatial structure (5).

Shortened equations for complex amplitudes of counterpropagating polarization waves

$$\left[\frac{\partial}{\partial\tau} + \Gamma_2 - i\Phi\right]p_+ = -in\alpha_+ - \frac{n_z}{2}\alpha_-,$$

$$\left[\frac{\partial}{\partial\tau} + \Gamma_2 - i\Phi\right]p_- = -in\alpha_- + \frac{n_z^*}{2}\alpha_+, \quad (9)$$

taking into account the shift $\Phi = (\omega_{21} - \omega_0)/\nu_c$ of the DFB Bragg frequency ω_0 relative to the frequency of the two-level transition ω_{21}, include nonlinear resonant scattering of counterpropagating waves on the complex population-inversion grating created by them.

The dynamics of the superradiant state of a laser with a low-Q combined cavity FP-DFB was studied using the numerical solution of nonlinear and linearized Maxwell–Bloch equations for various levels of homogeneous CW pumping n_p using the modified Runge–Kutta method of the 4th order and the grid method with the same boundary conditions at opposite ends of the cavity: $\alpha_+(-L/2) = R\alpha_-(-L/2)$

and $\alpha_-(L/2) = R\alpha_+(L/2)$. Only small noises of polarization of the active medium $|p_\pm| \sim 10^{-4}$ were set at the initial moment of time, and the electric field and the population-inversion grating were considered absent: $\alpha_\pm = 0$, $n_z = 0$, which, as it was verified, did not affect the characteristics of the steady-state lasing of interest to us, both stationary and non-stationary.

The following relaxation rates of polarization and population inversion were chosen as characteristic values of superradiant lasers: $\Gamma_2 = 2\Gamma_1 = 0.02 \ll \Gamma_E \lesssim 1$. Then, according to calculations, at the pump level n_p, which is sufficiently much higher than the first threshold of lasing $n_0 \approx \Gamma_2\Gamma_E$, counterpropagating superradiance pulses, that occur not quite simultaneously at the transition stage of the process spontaneously form a substantially inhomogeneous half-wavelength population-inversion grating. This grating can be not only stationary mirror-symmetric (below the second laser threshold, i.e. the limit for stationary lasing), but also non-stationary mirror-asymmetric, ensuring a strongly asymmetric radiation of a symmetrical laser in steady state. The latter state is characterized by a difference from the unit of the radiation-intensity asymmetry factor:

$$r = \max\left[\frac{|\alpha_\pm(\xi = \pm L/2)|^2|}{|\alpha_\mp(\xi = \mp L/2)|^2}\right]. \tag{10}$$

3. Self-modulation and multimode generation in superradiant lasers

First, taking into account the limited volume of the paper, we will qualitatively characterize the main mechanisms (scenarios) of non-stationary superradiant lasing, that we identified within the scope of the formulated model. At the end of the section the specific parameters of the model will be indicated, for which the following sections ensure a more detailed description of the properties of self-modulation and the radiation spectrum in typical laser operation.

I. First of all, like in conventional lasers with high-Q cavities [1–5], where $T_E^{-1} < T_2^{-1}$, the self-modulation in a single-mode operation, i.e., the oscillations of the amplitude and phase of one polariton mode, may be related primarily to the standard quadratic nonlinearity of saturation in the Bloch equations (8) for two-level active centers for the considered symmetric superradiant lasers if the second laser threshold is not exceeded significantly. In the case of an almost symmetrical profile of the main „central“ mode, modified by a self-consistent population-inversion grating, this self-modulation mechanism gives $r = 1$ and is especially effective in the conditions of excitation of one or several polariton sideband modes of the laser spectrum. The same quadratic nonlinearity is responsible for their resonant excitation in the absence of a positive growth rate, even at the level of population inversion up to n_p (allowed by pumping), i.e., exceeding the value $\langle \overline{n} \rangle_\tau$ averaged over the cavity and time in steady lasing that may be non-stationary. Indeed, it can result in excitation of consistent Rabi oscillations [1,15–17] of polarization in the equations for the field (7) according to eq. (9), if in a significant volume of the cavity the amplitude of the full field $\alpha = \alpha_+ \exp(ik_0z) + \alpha_- \exp(-ik_0z)$ ensures the frequency of the Rabi oscillations of population inversion $\Omega_R = dE/\hbar$ (i.e. $\Omega_R = |\alpha(\xi, \tau)|\nu_c\sqrt{\varepsilon_0}$) that is approximately equal to the frequency difference of any sideband and center modes. However, the implementation of such a self-modulated operation may require „fine tuning“ of the laser parameters, including its length and pumping level, since the inevitable mirror symmetrical grating of population inversion is a stabilizing factor, and the mechanism associated with the superradiance of periodic (see III) or irregular (see IV) pulses is primarily responsible for the destruction of the stationary state of the central polariton mode.

II. If the second threshold is greater exceeded in a wide range of laser parameters, the powerful central mode turns out to be strongly asymmetric due to the mirror-asymmetric location of the inhomogeneous consistent population-inversion grating, localized mainly near one of the mirrors even in a symmetrical cavity, and the asymmetry factor of laser radiation can be large: $r > 1$. The spatial structures of the central mode and the asymmetric grating oscillate synchronously in this case, which is more generic than I, i.e., they are subject to self-modulation owing to the same Rabi mechanism of excitation of less powerful polariton sideband modes. Counterpropagating waves of the latter practically do not experience resonant scattering on the specified grating, the spatial period of which differs from the period of their structure, and give almost mirror-symmetric radiation from a symmetrical cavity, which determines their inhomogeneous profile according to the difference in the reflection factor of mirrors R from 1 ($R \lesssim 0.5$). The discrete spectrum of laser radiation is typical for this and the previous cases and the sideband components of the spectrum can be located even outside the spectral line with a width of $2T_2^{-1}$, since the full width of the polariton spectrum of modes in a superradiant medium is limited only by the effective cooperative frequency [5,18] $\nu_c\sqrt{\langle \overline{n} \rangle_\tau}$ exceeding the value of T_2^{-1} in the considered cases of lasing.

III. The discrete spectrum is also ensured by another mechanism of the polariton-mode self-modulation associated with the highly nonlinear collective process of periodic lasing of Dicke superradiance pulses [5]. The fact is that after each pulse of mode superradiance emitted by a laser, the population inversion in a significant part of the active medium sharply becomes negative, and the field quickly exits the low-Q cavity. However, CW pumping during the time of the order of T_1 again creates everywhere, albeit relatively slowly, a positive population inversion. As a result, the reemittion of a superradiance pulse takes place, which can be regular and periodic, since it is induced not by random quantum or thermal noise (as in the well-known process of collective spontaneous Dicke superradiance), but by the field and polarization remaining in the cavity. Depending on their magnitude and structure, the superradiance pulses from opposite ends can be emitted synchronously or with a delay and can have different amplitudes, ensuring one or another modulation depth, not necessarily higher one, but on average maintaining the mirror symmetry of the radiation: $r = 1$.

IV. If, as in the second (II) mechanism, the polariton mode is mirror-asymmetric due to a consistent asymmetric population-inversion grating that is usually unsteady due to the Rabi-oscillation mechanism, then these forward and backward sequences of superradiance pulses can become generally asymmetric and, moreover, not strictly periodic, although they may remain regular to a certain degree. Then, a complex superposition of discrete and continuous spectra can be formed depending on the level of excitation of the sideband modes and the degree of coherence of the counter-propagating superradiance pulses, as well as on the degree of irregular deformation of the population- inversion grating by them. These spectra can be different at opposite ends of the laser, including in terms of average intensity ($r > 1$), and they also can be mirror-asymmetric with respect to the frequency of the central polariton mode, as a function of frequency. The latter mode is always represented in the spectrum as a narrow peak, and its width in most cases is much less than the width of the spectral line of the active medium $2T_2^{-1}$ (in the semi-classical approximation), although it may be of the order of $2T_2^{-1}$, especially in chaotic lasing of superradiance pulses (see below about the mechanism of VI and the example at the beginning of Sec. 5).

V. Another established self-modulation mechanism, also partially regular and resulting in the overlap of discrete and continuous spectra, arises due to irregular, random jumps of a highly inhomogeneous, localized population-inversion grating from one mirror to another and its rather long metastable existence near one or another mirror. Then the lasing can be quasi-periodic only at these separate metastable stages when the radiation asymmetry factor (10) $r_\nu(\tau)$ differs from one significantly, though on average it is equal to one. In general, the radiation oscillogram is a non-periodic sequence of sections of a fairly smooth variation of intensity and sections of short superradiance pulses partially partially synchronized at opposite ends only during the metastable stages.

VI. Finally, self-modulation becomes essentially chaotic usually when the laser threshold is very significantly exceeded, and the radiation spectrum becomes almost continuous and mirror-symmetric (both in frequency and in space, $r = 1$) in case of an interdependent destruction of the population-inversion grating and chaotic superradiance pulses of counterpropagating waves. In this case, the mechanism of self-modulation constitutes the disordered formation and reabsorption of virtually independent superradiance pulses of counterpropagating waves in the active medium. It corresponds to a spectrum in the form of a high smooth central peak with a width of the order of T_2^{-1} and a smooth pedestal with a width much larger than T_2^{-1}, but less than or of the order of $\nu_c\sqrt{n_p}$.

These mechanisms of self-modulation of laser radiation are modified in the range of parameters for which there is competition between two resonant spatial structures such as a given DFB and the resulting population-inversion grating. Usually, it results in a complication of the coexisting discrete and continuous spectra. Earlier studies of the superradiant steady-lasing spectra [7,16,17] in the absence of DFB showed that in the case of a symmetrical Fabry-Perot cavity, asymmetric emission almost always has a self-modulating character associated with the excitation of additional (sideband) polariton modes due to the mechanism II of nonlinear Rabi oscillations. It occurs when the condition $\Gamma_2 \ll \Gamma_E \lesssim \sqrt{n_p}$ is met, so that the pumping level significantly exceeds the laser threshold $n_0 = \Gamma_2\Gamma_E$. The asymmetry of the radiation is attributable to the formation of a self-consistent half-wavelength population-inversion grating, which at the same time plays both the role of an oscillating local Bragg mirror and the role of an amplifier. A wave traveling in one direction prevails over the counterpropagating wave and increases, taking almost all the pumping energy, and consequently, the radiation asymmetry factor r significantly increases. Naturally, in the case of a symmetrical Fabry-Perot cavity, the direction of the predominant laser emission is randomly selected with equal probability in both directions each time it is switched on, and in the future it either persists (stable scenario II) or occasionally switches (scenario V).

The establishment of the mechanisms (scenarios) of self-modulation superradiant lasing formulated above in this paper is based on a significant broadening of the cavity parameters used for modeling. For confirmation of the existence of these self-modulation mechanisms, Secs. 4 and 5 show the results of the analysis of an illustrative sample of the calculations performed, limited mainly by combinations of small sets of typical values of the reflection factor of mirrors $R = 0.2$, 0.7, the DFB coefficients $\beta = 0$, 0.001, 0.01, 0.2, the shifts of the Bragg frequency relative to the frequency of the laser transition $\Phi = 0$, 0.1, and pumping levels $n_p = 0.1$, 0.25, 0.5, 1. At the same time, the laser length $L = 2$ and the relaxation rate of polarization and population inversion $\Gamma_2 = 2\Gamma_1 = 0.02$ were fixed, and the calculated field-decay rate of the highest-Q mode did not differ much from the estimate $\Gamma_E \approx -(\ln R)/L$, which gives values of 0.8 and 0.18 at $\beta = 0$ for $R = 0.2$ and 0.7, respectively. The indicated values of Γ_E when taking into account the DFB even at $\beta = 0.2$, are refined only to $\Gamma_E \approx 0.7$ and 0.16, respectively, since the Bragg structure in the considered combined cavities additionally contributes only a small integral reflection factor $\beta L \leq 0.4$.

4. Lasing in a very low-Q cavity

The effect of DFB with a small coefficient $\beta \lesssim 0.01$ on the characteristics of steady lasing is very insignificant (no more than a few percent) for a low-Q cavity with weakly reflecting mirrors with $R = 0.2$, when the rates of relaxation

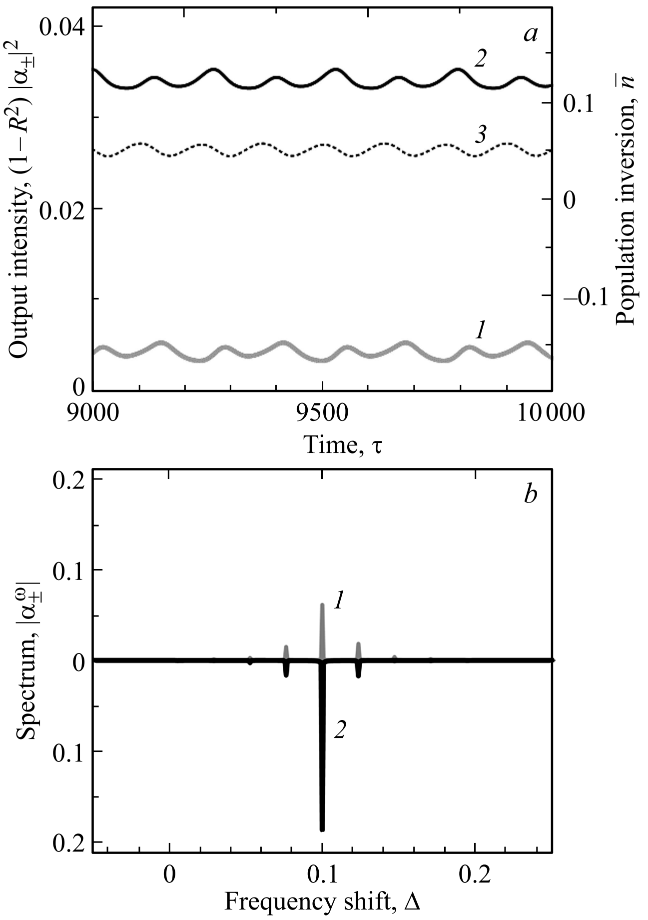

Figure 1. Self-modulation in a laser with a low-Q combined cavity with length $L = 2$, pumping $n_p = 1$, mirror reflection factor $R = 0.2$, DFB coefficient $\beta = 0.01$, shift of the center of the spectral line relative to the resonant Bragg frequency $\Phi = 0.1$: *a)* oscillograms of the intensity of the outcoming radiation of counterpropagating waves $(1 - R^2)|\alpha_\pm|^2$ (*1, 2*) and the average population inversion $\bar{n}(\tau)$ (*3*); *b)* — spectra $|\alpha_+^\omega|$ of a wave traveling to the right (light lines *1*), and spectra $|\alpha_-^\omega|$ of a wave travelling to the left (black lines *2*).

of polarization and field differ by many times and a laser threshold is low, $\Gamma_E \approx 40\Gamma_2$ and $n_0 \approx 0.016$. In this case the self-modulation mechanism II is implemented, regardless of the frequency shift Φ. Namely, at high pumping levels $n_p = 0.5$ and 1, a weakly modulated asymmetric lasing is realized with average factors $r \approx 3$ and 9 and increased average population inversion $\langle \bar{n} \rangle_\tau \approx 0.047$ and 0.05 and the amplitude of the stronger of the counterpropagating waves of the central mode $|\alpha_-^\omega| \approx 0.1$ and 0.17, respectively, instead of stationary symmetric single-mode lasing, which takes place, for example, at $n_p = 0.1$, when the average population inversion and equal amplitudes of outcoming counterpropagating monochromatic waves are $\bar{n} \approx 0.035$ and $|\alpha^\omega| \approx 0.03$ (Figure 1).

The modulation is almost harmonic and corresponds to the presence of two symmetrical sideband modes (harmonics), in amplitude about an order of magnitude weaker than the central mode, and their second harmonics, which are many times weaker. The frequency detuning of these sideband modes from the central mode practically does not change with a variation of the pumping level and is approximately equal to the frequency detuning of the central and two of the most high-Q polariton sideband modes $\Delta_\pm \approx \pm 0.023$, calculated on the basis of linearized equations with homogeneous population inversion, estimated as its average level in nonlinear simulations $\bar{n} \sim 0.05$. These detunings also weakly depend on the shift Φ of frequency of the laser transition relative to the DFB Bragg frequency, which is taken equal to the frequency of one of the partial modes of the Fabry-Perot cavity. The fact is that the spectral width $2\Gamma_E \approx 1.6$ of such partial modes is of the order of the intermode distance $\pi/L \approx 1.6$ and their electromagnetic field contributes only small fraction of energy of polariton modes compared to the polarization of active medium [18]. In general, the field of the central polariton mode is decisive and according to [5,7,16,17] and what was said in Sec. 3, supports an asymmetric population-inversion grating $n_z(\xi, \tau)$ as well as creates with its help undamped Rabi oscillations of active centers that excite sideband modes due to the quadratic nonlinearity of the medium. The asymmetric grating makes strongly asymmetric the nonlinear consistent structure of the central mode and the radiation emitted by it from opposite ends, whereas the radiation of the sideband modes, which do not experience the resonant action of the grating, essentially has a mirror symmetry (Figure 1, *b*).

It should be noted that the occurrence of self-modulation at $\Phi = 0.1$, albeit very weak, but with approximately the same period $\tau_m = \pi/|\Delta_\pm| \approx 130$, takes place at a pumping level which is slightly less than 0.25 (for $\beta = 0.01$) and corresponds to the mechanism (scenario) I with $r = 1$. It gives mirror-symmetric radiation with wave amplitudes $|\alpha_+^\omega| = |\alpha_-^\omega| = 0.056$ at $n_p = 0.25$. However, in the case $\Phi = 0$ and the same pumping level, a strictly stationary lasing takes place, which is also symmetrical of course, but with a slightly larger amplitude of the polariton mode $|\alpha^\omega| = 0.065$, despite the previous level of average population inversion $\bar{n} = 0.043$. The specified estimate $\sqrt{\bar{n}}$ of the width of the spectrum of excited polariton modes is comparable to the shift $\Phi = 0.1$, which explains the noted difference in the laser operation in two cases $\Phi = 0.1$ and $\Phi = 0$.

Even a weak DFB with a coefficient of $\beta \lesssim 0.01$ (which practically does not affect the Q-factor of the modes), as well as a shift Φ of the frequency of the laser transition relative to the partial frequency of the Fabry-Perot cavity (and, hence, the DFB resonance) affect the asymmetry, amplitude, and degree of localization of the population-inversion grating near one of the mirrors, reducing the asymmetry factor of radiation r by the value of $\sim 10\%$ at the maximum pumping level $n_p = 1$ (at $\beta = 0$ the factor $r = 9.2$). The competition between the DFB and the consistent grating becomes stronger with higher coefficient β and can result in its unsteady dissection and delocalization, and therefore the symmetrization of laser radiation.

For instance, in the case $\beta = 0.2$ a transition occurs according to mechanism I, to a very significant, 30 percent modulation of the intensities of outcoming counterpropagating waves for both frequency shifts $\Phi = 0$ and $\Phi = 0.1$ discussed above with a change of pumping from the level $n_p = 0.1$, when stationary lasing is implemented (with approximately the same values $\bar{n} \approx 0.035$ and $|\alpha^{\omega}| \approx 0.03$, as with $\beta = 0.01$), up to the level of $n_p = 0.25$. This modulation is symmetrical, but significantly anharmonic with a period $\tau_m = 2\pi/|\Delta_{\pm}| \approx 280$ and approximately the same frequency detuning of the sideband modes $\Delta_{\pm} \approx \pm 0.022$ from the central mode, having approximately the same amplitude $|\alpha^{\omega}| \approx 0.06$ with the same average population inversion $\langle \bar{n} \rangle_{\tau} \approx 0.045$, as in the above case $\beta = 0.01$. However, such modulation for the latter case was achieved only under conditions of strong pumping $n_p \sim 0.5-1$.

Now, with $\beta = 0.2$, a partial destruction of periodic oscillations and the regular structure of the population-inversion grating $n_z(\xi, \tau)$ takes place under the conditions of strong pumping, so that a combination of mechanisms IV and V is verified, and the time-average laser radiation becomes symmetrical ($r = 1$) in accordance with the latter mechanism. Simulations show that the discrete spectrum is significantly enriched and even suppressed by a continuous spectrum having a width of the order of the effective cooperative frequency $\sqrt{\langle \bar{n} \rangle_{\tau}} \approx 0.25$ and turns out to be asymmetric with respect to the frequency of the central polariton mode, which corresponds to a single well-defined line with a width significantly less than $\Gamma_2 = 0.02$. At the same time, the relative modulation of the radiation intensity can reach tens of percent (and even exceed the average value many times during the emission of individual superradiance pulses with a duration of $\sim 3-10$, i. e., of the order of the inverse effective cooperative frequency) at long stages of steady lasing with a duration of $\sim 300-1000$, i. e., of the order of several times T_1. Deviations from the mirror symmetry of laser radiation turn out to be higher at quieter stages of such lasing and can be of the order of $10-20\%$, having an equal probability of the prevalence of emission through one or another end. However, the laser can emit almost the same quasi-periodic regular radiation from opposite ends for some sets of parameters, for example, with $\Phi = 0$ and $n_p = 0.5$, smoothly varying in intensity by the amount of $\sim 30\%$, having two main periods ~ 100 and ~ 700 and corresponding to the variable delay of the maxima of outcoming modulated counterpropagating waves for the time $\sim 30-100$.

According to simulation the self-modulation mechanisms II and III with a discrete spectrum are realized in the case of symmetric (and also almost symmetric) cavities with $R \approx 0.5$ and $\beta \lesssim 0.01$ at the following pumping levels: $n_p \sim 0.5-1$ for mechanism II, when two sideband modes with frequency detuning $|\Delta_{\pm}| = \pi/\tau_m \approx 0.036-0.037$ are excited and there is a large asymmetry of the emitted radiation with a factor $r \sim 4-10$, and $n_p \sim 0.1$ for mechanism III, when the spectrum contains about 10 equidistant harmonics with a step of $\Delta_m = 2\pi/\tau_m \approx 0.05$ and corresponds to the repetition period of $\tau_m \approx 125$ of symmetrically emitted ($r = 1$) superradiance pulses. In this case, the lasing is stationary symmetric closer to the laser threshold $n_0 \approx 0.007$, more precisely, at $n_p \lesssim 0.05$, and it is symmetrical, on average, at moderate pumping $n_p \sim 0.25$ but with a significant continuous component in the spectrum owing to the incessant irregular switching between the lasing of superradiance pulses and the lasing of a quasi-stationary asymmetric polariton mode. The description of these cases (modes) is omitted because of the limited scope of the article.

5. Lasing in a moderate-Q cavity

An increase of the reflection factor of mirrors by 3.5 times to $R = 0.7$ makes the width of the partial mode of the Fabry-Perot cavity equal to $2\Gamma_E \approx 0.36$, i. e. 4.5 times less than the intermode distance $\pi/L \approx 1.6$, and significantly enriches the dynamics of the laser. Its characteristics turn out to be significantly different compared to the characteristics discussed in the previous section and are more sensitive to the frequency shift Φ, although they still change slightly (by the amount of $\lesssim 10\%$) with a change of the DFB coefficient if it is small, $\beta \lesssim 0.01$.

In this case, at a zero shift $\Phi = 0$, the scenario (mechanism) III of periodic lasing of identical forward and backward sequences of superradiance pulses is realized above the second laser threshold, (with the average population inversion: $\langle \bar{n} \rangle_{\tau} \sim 0.04$, instead of stationary lasing, which takes place with a low population inversion $\bar{n} \sim 0.01$ between the first ($n_0 \approx 0.004$) and the second (an order of magnitude larger than n_0) laser thresholds. For instance, at the pumping level $n_p = 0.1$, the mean value $\langle \bar{n} \rangle_{\tau} = 0.036$ and the instantaneous population inversion $\bar{n}(\tau)$ for each period of duration $\tau_s = 166$ smoothly increases from $\min(\bar{n}) = 0.017$ to $\max(\bar{n}) = 0.05$, and then it drops sharply to the same minimum during the flash of the pulse $\tau_i = 36$. It sets the half-width $2\pi/\tau_i \approx 0.2$ of a discrete radiation spectrum containing about 10 equidistant harmonics.

The average population inversion increases to $\langle \bar{n} \rangle_{\tau} \sim 0.05-0.07$ at a higher pumping level $n_p \sim 0.25-0.5$, the pulse emission becomes almost random, following the mechanism VI, but it is implemented with breaks. The mechanism of metastable switching of the asymmetric population-inversion grating is additionally activated during this „break“ time intervals. At the episodic stages of the quasi-stationary existence of the grating, the asymmetry of the smoothly varying radiation is small, of the order of $10-20\%$, and these stages themselves account for not more than 50% of the lasing time. The total spectrum is continuous with a width of ~ 0.5 and has one central peak with a width of ~ 0.03, i. e. $\sim \Gamma_2$.

The mechanism II works at the pumping level $n_p = 1$: the population-inversion grating is well localized and is always located near one of the mirrors, although it quasi-periodically oscillates along with oscillations of the outgoing

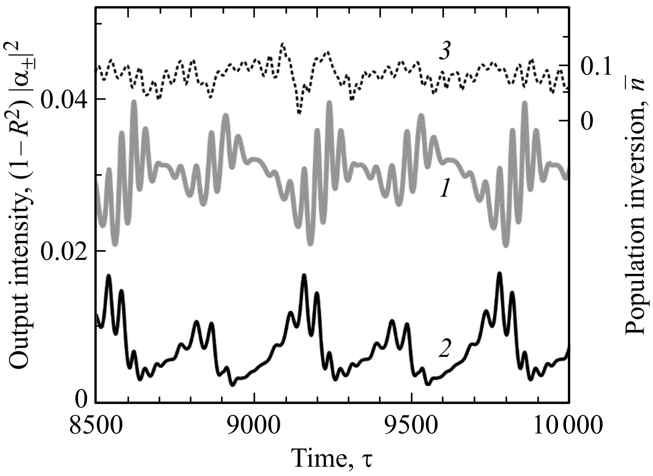

Figure 2. Self-modulation in a laser with a moderate-Q cavity of length $L = 2$, pumping $n_p = 1$, mirror reflection factor $R = 0.7$, DFB coefficient $\beta = 0.001$ and the center of the spectral line coinciding with the resonant Bragg frequency, $\Phi = 0$. The oscillograms of the intensity of the outcoming radiation of the counterpropagating waves $(1 - R^2)|\alpha_\pm|^2$ are shown by the light line (*1*) for the wave α^+ travelling to the right, and by the black line (*2*) for the wave α_- travelling to the left; the average population inversion $\bar{n}(\tau)$ is shown by a dashed line (*3*).

radiation, the intensities of which differ on average by $r = 4.5$ times at opposite ends (Figure 2). In this case, the mean value $\langle\bar{n}\rangle_\tau = 0.075$, there are no superradiance pulses, the discrete spectrum is more pronounced than the continuous spectrum and the peak of the central mode is narrowed to ~ 0.002, i. e. $\sim 0.1\Gamma_2$.

The range of pumping levels ensuring stationary single-mode generation expands to $n_p \sim 0.1$ for lasers with a non-zero frequency shift $\Phi = 0.1$ and a small DFB factor $\beta = 0.01$, and the average population inversion reaches the value of $\bar{n} = 0.03$ at $n_p = 0.1$. The mechanism I works for pumping with a higher level $n_p = 0.25$, which leads to an almost twofold increase of the average value of $\langle\bar{n}\rangle_\tau = 0.054$ and deep harmonic modulation of symmetrical laser radiation with a relative change of intensity of $\pm 40\%$ and a short period $\tau_m = 2\pi/|\Delta_\pm| \approx 48$. Here, the population-inversion grating $n_z(\xi, \tau)$ is mirror symmetric, and its spectrum, as well as the field spectrum, are discrete and contain only two harmonics with detunings $\Delta_\pm \approx \pm 0.13$ on the sidebands of the central mode.

This situation is shown in Figure 3 for typical characteristic pumping levels, where the amplitude spectra $|\alpha_-^\omega|$ of the wave approaching the left mirror are demonstrated. Namely, the discrete spectrum is enriched at $n_p = 0.5$ and $n_p = 1$, remaining almost symmetrical and quasi-equidistant and almost without changing its width (approximately equal to the effective cooperative frequency $\sqrt{\langle\bar{n}\rangle_\tau} \approx 0.27$), and is also slightly complemented by a continuous spectrum. There are no superradiance pulses in these two cases, but the spectra, dynamics and asymmetry of the radiation are different in structure and origin.

The first case $n_p = 0.5$ represents a self-modulation mechanism V with an almost periodic transition of a completely localized population-inversion grating from the left mirror to the right and back during the time $\tau_m = 2\pi/\Delta m \approx 760$ (therefore, on average, the laser emits symmetrically, $r = 1$). There are 14 smooth peaks of radiation of outcoming counterpropagating waves at each such period. It is corresponds to the presence of two sideband harmonics in the spectrum with detunings $\Delta_\pm = \pm 2\pi/\tau_\pm \approx 0.058$ from a narrow central polariton mode.

The second case $n_p = 1$ represents mechanism II with the radiation asymmetry factor $r = 4.85$, almost 10% higher than this factor in the Fabry-Perot cavity; cf. variant with $\beta = 0.001$ and $\Phi = 0$ above. The oscillogram of fields and population inversion turn out to be qualitatively the same as in that variant. Again, the population-inversion grating is well localized, constantly located near one of the two mirrors, without moving to the other, and quasi-periodically oscillates in accordance with the outcoming radiation, demonstrating two periods of oscillation. Of these, the smaller one is ~ 7 times shorter than the larger $\tau_m = 2\pi/\Delta_m \approx 320$, which explains the quasi-equidistance of the spectrum with a step of $\Delta_m \approx 0.02$ (Figure 3).

Finally, let us turn to the laser that has a combined cavity with a significant DFB coefficient $\beta = 0.2$, which significantly affects the dynamics.

In this variant, the parameters of stationary lasing within the entire pumping range up to the second laser threshold, including the case of $n_p = 0.1$, remain practically the same as in the previous variant at $\beta = 0.01$, and even, unlike

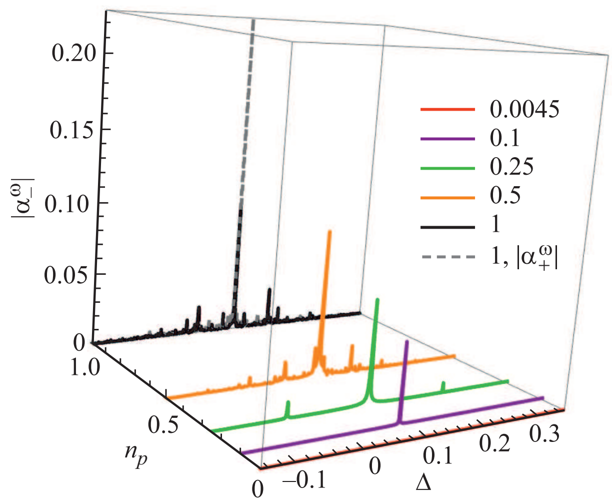

Figure 3. Spectra of a wave α_-^ω traveling to the left in steady operation of a laser with a length $L = 2$, mirror reflection factor $R = 0.7$, DFB coefficient $\beta = 0.01$, shift of the center of the spectral line relative to the resonant Bragg frequency $\Phi = 0.1$ for different pumping levels n_p: 0.1 (purple line), 0.25 (green), 0.5 (orange), 1 (black); in the latter case, the spectrum of the counterpropagating wave $|\alpha_+^\omega|$ is shown by a gray dashed line. Red line indicates the pumping threshold level $n_0 = 0.0045$. (A color version of the figure is provided in the online version of the paper.)

it, do not differ for different frequency shifts $\Phi = 0$ and $\Phi = 0.1$. However, the differences are cardinal at the pumping level $n_p = 0.25$, except for the almost constant average population inversion $\langle \overline{n} \rangle_\tau \approx 0.06$. For $\Phi = 0$, the combination of mechanism of switching V and chaotic superradiance VI is replaced by the mechanism I, namely strictly harmonic self-modulation with depth $\pm 15\%$ and period $\tau_m = 2\pi/|\Delta_\pm| \approx 80$, giving two sideband harmonics in the spectrum with detuning $\Delta_\pm \approx \pm 0.079$ from the frequency of the polariton mode. For $\Phi = 0.1$, such harmonic modulation in mechanism I acquires a complex quasi-periodic form with a large depth $\pm 60\%$, a long period $\tau_m = \pi/|\Delta_m|$ of about 260 and a short period of about 83. In general, the spectrum is almost discrete and equidistant, including the polariton mode and a dozen harmonics with a step of $\Delta_m \approx 0.024$.

At the pumping level $n_p = 0.5$, qualitatively similar self-modulated operation is implemented for shifts $\Phi = 0$ and $\Phi = 0.1$, following the mechanism of random switching V and giving almost the same average population inversion $\langle \overline{n} \rangle_\tau \approx 0.073$ and short (with duration $\sim 100-300$) frequent episodes of a small ($\sim 10\%$) violation of the mirror symmetry of radiation ($r_v = 1.1-1.2$). However, here, there are no pronounced superradiance pulses unlike the variant with $\beta = 0.01$, i. e., additional action of the mechanism VI is absent.

Finally, the mechanism V of random transition of such an asymmetric grating from one mirror to another continues to operate at pumping level $n_p = 1$, in contrast to the case of small value $\beta = 0.01$, when there is an essential part of the mechanism II of quasi-periodic Rabi oscillations of the population-inversion grating localized at one of the mirrors. At the same time, the change of the shift between the frequencies of the laser transition and the Bragg resonance DFB from $\Phi = 0$ to $\Phi = 0.1$ preserves the mirror symmetry of the radiation on average ($r = 1$) and is accompanied by:

1) a drop of the average population inversion $\langle \overline{n} \rangle_\tau$ from a value of 0.074 (also characteristic of both variants at $n_p = 0.5$) to a value of 0.056 (characteristic of them at $n_p = 0.25$);

2) an almost twofold reduction of the average duration of episodes of asymmetric radiation with a prevalence of emission to the right or left from the value ~ 300 to the value ~ 150;

3) an increase of the average value and spread of the radiation asymmetry factors r from $4-5$ to $5-10$ in a separate such episode with a quasi-stationary population-inversion grating;

4) a significant increase of the number (at almost the same typical amplitude) of superradiance pulses, especially pronounced in the periods between these episodes;

5) a significant broadening of discrete components in the spectrum, i. e., the predominance of a continuous spectrum, as well as an increase of its width from about 0.3 to almost 0.5.

The oscillograms of the emitted counterpropagating waves and the spatiotemporal dynamics of the population-inversion grating, characteristic of the switching self-modulating mechanism (scenario) V, are shown in Figure 4 for the value of the DFB coefficient $\beta = 0.1$, the frequency shift $\Phi = 0.1$ and the highest pumping level $n_p = 1$.

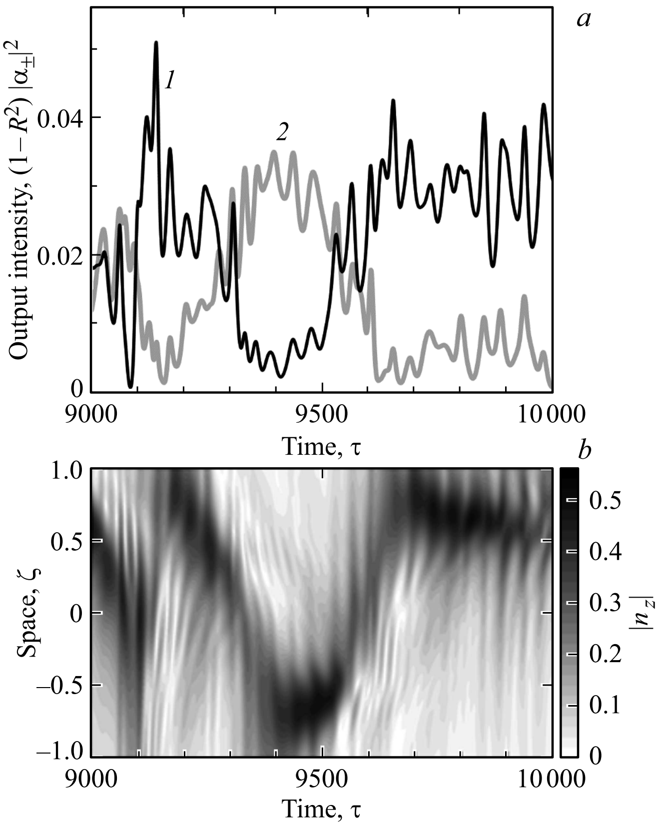

Figure 4. Switching in a laser with length $L = 2$, pumping level $n_p = 1$, mirror reflection factor $R = 0.7$, DFB coefficient $\beta = 0.01$, shift of the center of the spectral line of the active medium relative to the resonant Bragg frequency $\Phi = 0.1$: *a)* oscillograms of the intensity of outcoming radiation of counterpropagating waves $(1 - R^2)|\alpha_\pm|^2$; *b)* spatio-temporal evolution of the amplitude modulus of the population-inversion grating $|n_z|$.

6. Conclusion

Thus, the main mechanisms and forms of self-modulation of the outcoming radiation, generally mirror-asymmetric, as well as its spectra, generally containing discrete and continuous components are described, for a superradiant laser with a symmetrical low-Q combined Fabry-Perot (FP) cavity with distributed feedback (DFB) of counterpropagating waves. Namely, typical mechanisms of self-modulation of the main laser polariton mode are excitation of neighboring polariton modes due to Rabi oscillations, enrichment of the discrete spectrum with quasi-equidistant harmonics due to quadratic nonlinearity or nonlinearity of collective Dicke superradiance, expansion of the continuous part of the spectrum due to dissipative (radiative) instability or desynchronization of pulsed superradiance of counterpropagating waves.

It is shown that the self-modulation of steady lasing and its spectrum, as well as the radiation asymmetry factor r, equal to the ratio of radiation intensities from opposite ends of the laser, are largely determined by the space-time structure of a self-consistent population-inversion grating. It is also significant that the scattering and amplification of counterpropagating waves of the main polariton mode on this inhomogeneous grating competes with their scattering on a distributed feedback structure set by a cavity and affects both the properties of a regular or irregular sequence of superradiance pulses and the structure and dynamics of this central mode of the spectrum. These mechanisms of self-modulation of laser radiation are modified if, in a certain range of parameters, such competition of two resonant spatial structures takes place, which usually results in the complication and overlap of discrete and continuous spectra.

The most important control parameters are: mirror reflection factor R, DFB coefficient β, shift Φ of the center of the spectral line of the active medium relative to the resonant Bragg frequency of DFB, length L of the FP-DFB cavity and the CW pumping level n_p. These values depend on: the established nature of the generated superradiance pulses of counterpropagating waves, the self-modulation of the main, central polariton mode and the characteristics of the remaining, sideband polariton modes, which can be excited due to resonant Rabi oscillations of active centers in its strong field. Extensive possibilities for controlling the properties of coherent radiation and its spectrum in superradiant lasers are demonstrated by means numerical simulations. In particular, it is shown that it is possible to control the characteristics of simultaneous generation of one powerful strongly asymmetric mode in the center of the spectral line of active medium and a number of weaker modes (harmonics) beyond it, emitting almost mirror-symmetrical radiation.

It should be noted that the demonstrated lasing features are far from exhausting the dynamics of superradiant lasers. Questions remain open about how the dynamics are affected by the length of the laser, the asymmetry of its cavity, the spatially inhomogeneous profile of CW pumping, the inhomogeneous broadening of the spectral line of the active medium, its relationship with the relaxation rates of dipole oscillations and population inversion of active centers, and other parameters. In addition, the question of the actual width of spectral bands formed by individual modes (harmonics) may require the development of the quantum theory of a superradiant laser.

Further study of the mechanisms of formation and stable existence of various spatiotemporal patterns of superradiant states for a system of many particles with radiation interaction in a low-Q cavity is of interest from the point of view of both the fundamental physics of dissipative (dynamic) phase transitions and the applied physics of self-organizing laser-type systems with CW pumping.

Funding

This study was supported financially by the Russian Science Foundation (project 21-72-30027).

Conflict of interest

The authors declare that they have no conflict of interest.

References

[1] Ya.I. Khanin, Prinsiples of Laser Dynamics (North Holland, 2012).
[2] T. Erneux, P. Glorieux. *Laser Dynamics* (Cambridge University Press, 2010).
[3] P. Peterka, P. Koška, J. Čtyroký. IEEE J. Select. Top. Quant. Electron., **24**, 902608 (2018).
[4] L. Lugiato, F. Prati, M. Brambilla. *Nonlinear Optical Systems* (Cambridge: Cambridge University Press, 2015).
[5] A.M. Samson, L.A. Kotomtseva, N.A. Loiko. *Avtokolebaniya v lazerakh* (Minsk, Navuka I tekhnika, 1990). (in Russian).
[6] Vl.V. Kocharovsky, V.V. Zheleznyakov, E.R. Kocharovskaya, V.V. Kocharovsky, Phys. Usp, **60**, 345 (2017).
[7] E.R. Kocharovskaya, A.V. Mishin, Vl.V. Kocharovsky, V.V. Kocharovsky. Semicond., **56**, 333 (2022).
[8] K. Cong, Q. Zhang, Y. Wang, G.T. Noe II, A. Belyanin, J. Kono. JOSA B, **33**, 80 (2016).
[9] T.S. Mansuripur, C. Vernet, P. Chevalier, G. Aoust, B. Schwarz, F. Xie, C. Caneau, K. Lascola, Chung-en Zah, D.P. Caffey, T. Day, L.J. Missaggia, M.K. Connors, C.A. Wang, A. Belyanin, F. Capasso. Phys. Rev. A, **94**, 063807 (2016).
[10] W. Zhang, E.R. Brown, A. Mingardi, R.P. Mirin, N. J ahed, D. Saeedkia. Appl. Sci., **9**, 3014 (2019).
[11] E.Y. Paik, L. Zhang, G.W. Burg, R. Gogna, E. Tutuc, H. Deng. Nature, **576**, 80 (2019).
[12] Zhang Wu, Yu Chen, Hui Zhai. Sci. Bulletin, **63**, 542 (2018).
[13] Q. Wu, Y. Zhang, X. Yang, S.-L. Su, Ch. Shan, Klaus Mulmer. Sci. China Phys. Mech. Astron., **65**, 217311 (2022).
[14] D. Botez, M.A. Belkin. Eds., *Mid-Infrared and Terahertz Quantum Cascade Lasers* (Cambridge University Press, 2023).
[15] L. Allen, J.H. Eberly. Optical Resonance and Two-Level Atoms, Dover Publications Inc., N.Y. (1975).
[16] E.R. Kocharovskaya, Vl.V. Kocharovsky, V.V. Kocharovsky. Radiophys & Q.Electron., **66**, 167 (2023).
[17] E.R. Kocharovskaya, V.V. Kocharovsky. Semicond., **57**, 337 (2023).
[18] V.V. Zheleznyakov, Vl.V. Kocharovskii, V.V. Kocharovskii. Sov. Phys. Usp, **159**, 835 (1989).

Translated by A.Akhtyamov